

Molecular commensurability with a surface reconstruction: STM study of azobenzene on Au(111)

A. Kirakosian, M. J. Comstock, Jongweon Cho, and M. F. Crommie

*Department of Physics, University of California at Berkeley, Berkeley, California 94720, USA
and Materials Sciences Division, Lawrence Berkeley National Laboratory, Berkeley, California 94720, USA*

(Received 1 October 2004; revised manuscript received 21 December 2004; published 23 March 2005)

Azobenzene derivatives form a unique class of photoactive molecules that have the potential for nanoscale optical applications. We have observed the self-assembly behavior of azobenzene molecules adsorbed to Au(111) using scanning tunneling microscopy (STM). We find that azobenzene creates a surprising variety of surface structures whose commensurability with the underlying Au(111) “herringbone” reconstruction is coverage dependent. Two commensurate molecular chain phases exist in the low-coverage regime, and phase conversion between these structures can be induced using the STM tip. In the high-coverage regime we observe incommensurate molecular phases as well as commensurate molecular vacancy ordering. These molecular structures reflect a coverage-dependent competition between molecule-molecule and molecule-substrate interactions.

DOI: 10.1103/PhysRevB.71.113409

PACS number(s): 68.43.Hn, 68.37.Ef, 82.30.Nr, 81.16.Dn

Engineering the self-assembly and functional characteristics of adsorbed molecules is critical for laying the groundwork of future nanotechnologies. Progress has been made in this direction using molecular classes that exhibit polar functional behavior,^{1–6} chirality,^{7,8} “spacer leg” groups,^{9–11} and different optical properties.^{12–14} Azobenzene is an important member of this final class because it undergoes a reversible, photoactive *trans-cis* isomerization that may allow it to serve as an optically active device element.^{15,16} This simple molecule consists of two phenyl rings joined by a pair of double-bonded nitrogen atoms [Fig. 1(a) inset]. Some attempts have been made to observe the *trans-cis* isomerization of azobenzene-containing films with scanning tunnel microscopy (STM),^{17–19} but none have clearly resolved intramolecular structure, namely the phenyl rings.

In this paper, we resolve the intramolecular structure and self-assembly behavior of surface-adsorbed azobenzene molecules. We find that azobenzene molecules deposited onto Au(111) form a surprising variety of molecular structures whose commensurability with the periodicity of the underlying Au(111) herringbone surface reconstruction depends on molecular coverage. At low coverage we observe two commensurate molecular chain phases that can be converted, one to the other, via manipulation with the STM tip. At saturation coverage the azobenzene molecules switch to an incommensurate configuration comprised of two new phases. Commensurability is regained, however, at only slightly lower coverages as molecular *vacancies* order with the underlying herringbone reconstruction. This behavior arises from a coverage-dependent competition between intermolecular and molecule-substrate interactions for azobenzene on Au(111).

We performed our measurements using a home-built variable-temperature UHV STM (base pressure $<5 \times 10^{-11}$ Torr). A clean Au(111) substrate was obtained by repeated cycles of Ar-ion sputtering and annealing. Azobenzene molecules were leaked into the vacuum chamber and deposited onto the Au(111) substrate at room temperature. After azobenzene exposure, the sample was transferred to the STM, which was operated between 35 K and room temperature. At room temperature, azobenzene molecules diffuse and

are too unstable for STM imaging. At saturation coverage [one monolayer (1 ML)] azobenzene is stable enough for imaging at 90 K, while lower coverage structures (0.5–0.8 ML) required cooling to 35 K. Tunneling currents were kept below 100 pA for stable imaging.

Figure 1(a) shows a 0.50 ML coverage of azobenzene on the Au(111) surface. The Au(111) herringbone reconstruction consists of parallel pairs of slightly elevated surface ridges²⁰ [outlined by the dashed lines in Fig. 1(a), parallel ridges separated by 6.3 nm] that separate domains of fcc- and hcp-ordered Au surface atoms. We can distinguish two types of azobenzene ordering relative to the herringbone reconstruction. The first, referred to as the “zigzag” phase, consists of long, zigzagging azobenzene chains that lie predominantly within the contours of the hcp regions of the herringbone reconstruction. The second phase, the “straight” phase, consists of straight azobenzene chains that run in the two directions oriented 120° from the ridges of the herringbone domain walls. Parallel straight chains appear to repel each other, having a minimum separation of 0.5 nm. Straight chains occasionally cross the herringbone ridges to form extended domains, as seen in the center of Fig. 1(a). The straight and zigzag phases alternate over much of the surface, and coexist even when the sample is cooled slowly from room temperature down to 35 K over a period of many hours.

We are able to convert the straight phase into the zigzag phase by imaging the azobenzene-coated surface at increased sample biases. This can be seen in Figs. 1(b) and 1(c), which show conversion from the azobenzene straight phase to the azobenzene zigzag phase after repeated STM scans. The straight chain domains of the initial image almost completely convert into zigzag domains filling both the fcc and hcp regions of the herringbone reconstruction. The transformation is irreversible and independent of the scan direction. The onset voltage for the transformation ranges from –1.5 to –2.0 V, and varies with changes to the tip apex. Tip-induced current and electric field perturb the molecules beneath the tip, freeing them to diffuse and rearrange. Limited

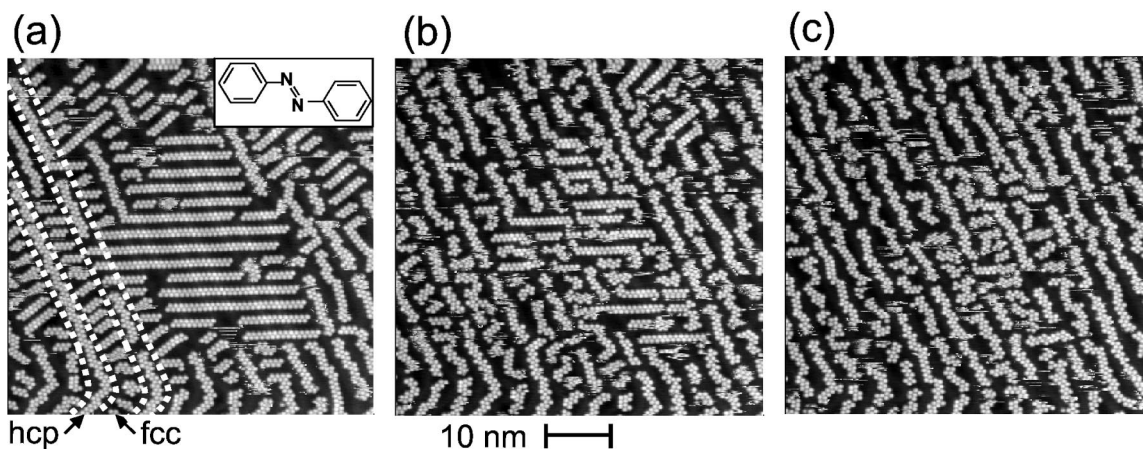


FIG. 1. STM images of 0.50 ML of azobenzene on Au(111) surface acquired at a typical scan bias of -1.25 V (59×59 nm, 50 pA, 35 K). The sequence from (a) to (c) shows the tip-induced conversion of the straight phase to the zigzag phase induced by scans at an elevated bias (-1.75 V). Inset to (a): the structural formula of the *trans* form of azobenzene.

thermal diffusion at 35 K results in the creation of the locally disordered zigzag phase.

The internal structure of the molecular chains can be more clearly seen in Fig. 2(a), which shows a close-up of a straight phase chain. The chain appears as eight closely spaced protrusions whose center-to-center spacing (~ 0.8 nm) in the marked directions is similar to the center-to-center spacing of phenyl rings in crystalline *trans*-state azobenzene (0.63 nm).²¹ Line scans taken across the chain [Fig. 2(b)] show that the depths of the minima between protrusions along the long-chain axis (*A-B*) are 45% greater than along the short-chain axis (*C-D*). This suggests that the protrusions along the short-chain axis are bonded differently than along the long-chain axis. We commonly observe chain lengths change spontaneously during scanning, always with pairs of protrusions attaching or detaching from the chain ends (often leading to an *odd* number of protrusions along the chain length). Hence, we identify adjacent pairs of protrusions along the short chain axis to be individual azobenzene molecules as shown in the Fig. 2(a) overlay. Isolated azobenzene molecules having the same shape as chain members have been observed at even lower coverages. We note that the azobenzene “dumbbell” appearance is similar to the related stilbene molecule that has been observed in films on the Ag/Ge(111)- $\sqrt{3}$ surface²² (with a similar center-to-center lobe distance of ~ 0.76 nm).

At higher molecular coverage (1 ML), where the Au(111) surface is saturated with azobenzene, we observe two different molecular orderings [marked I and II in Fig. 3(a)] that are incommensurate with the herringbone reconstruction. Phase I, shown more closely in Fig. 3(b), is a closed-packed structure where the positions of azobenzene phenyl lobes lie on a slightly distorted hcp lattice. The closed-packed arrangement of the phenyl lobes makes it difficult to be certain of the positions and orientations of individual azobenzene molecules within the film. The molecular arrangement sketched in the inset of Fig. 3(b) represents one of many possible arrangements. Phase II, shown more closely in Fig. 3(c), arranges the azobenzene molecules in a crisscross fashion. Phase II has a lower packing fraction than phase I and is

observed less often. Unlike phase I, the positions and orientations of individual azobenzene molecules in phase II are distinguishable [Fig. 3(c) inset].

Commensurability with the herringbone reconstruction is regained at slightly lower coverage ($\sim 20\%$ below the phase I saturation coverage) through an ordered vacancy structure that extends across the molecular layer. This can be seen in Fig. 4 where dark vacancies (typically the size of a single azobenzene molecule) orient themselves in either of the two

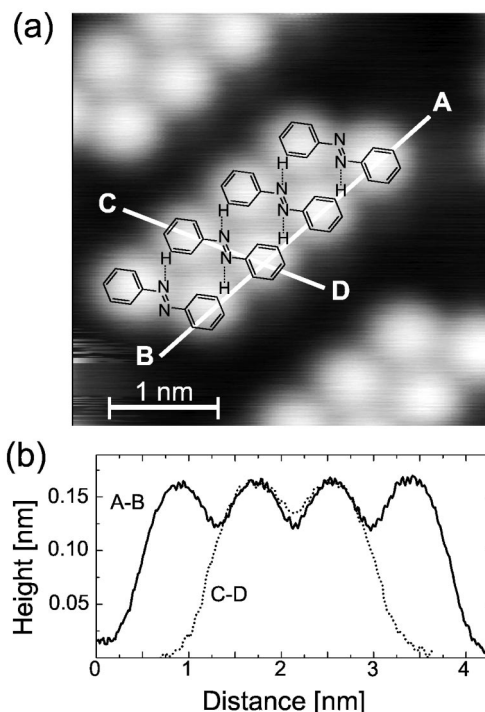


FIG. 2. (a) Close-up STM image of a short chain of azobenzene molecules confined to the fcc region of the Au(111) herringbone surface reconstruction (5×5 nm, -1.25 V, 50 pA, 35 K). Proposed molecular structure indicated by overlay (dotted lines represent hydrogenlike bonds). (b) Cross-sectional topographic line scans along the directions marked in (a).

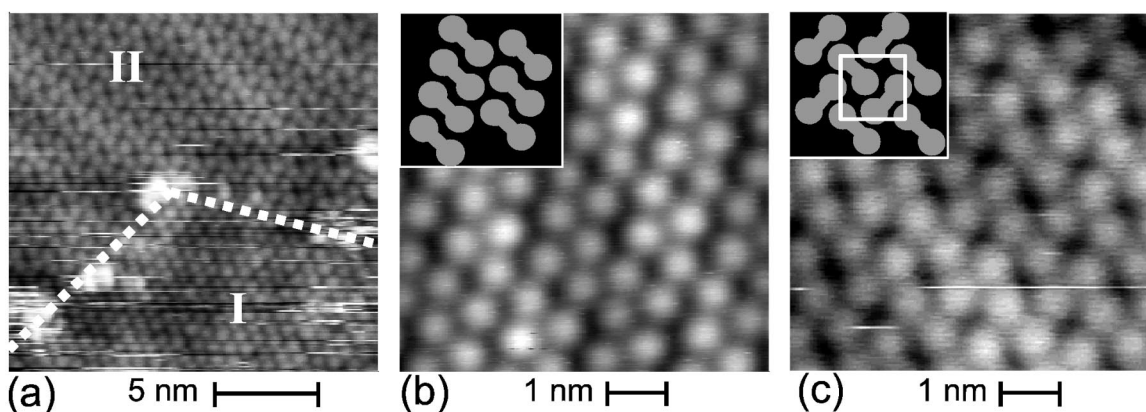


FIG. 3. STM images of the saturation coverage (~ 1 ML) of azobenzene on Au(111) surface (1.5 V, 25 pA, 90 K). (a) Large-scale image (18×18 nm) shows coexistence of two incommensurate phases, labeled I and II. The dashed line marks phase boundary. (b) Close-up image of phase I (6×6 nm). Inset: a diagram of a possible phase I molecular arrangement. (c) Close-up image of phase II (6×6 nm). Inset: the diagram of the phase II molecular arrangement with the unit cell marked by white box overlay.

directions 120° from the herringbone domain walls. The oriented vacancies form domain structures as outlined in the Fig. 4 overview image. Close-up images of the vacancy structure (inset) show that molecular segments four units long exist between the ordered vacancies.

The ordering of azobenzene molecules on the Au(111) surface is determined by the interplay of intermolecular and molecule-surface interactions. At low coverage, intermolecular interactions, which likely arise from a dipole-dipole interaction enhanced by hydrogenlike bonds, dominate short-range order. The hydrogenlike bond is formed between the unshared electron pair of a nitrogen atom of one azobenzene molecule and the net positive hydrogen atoms of the phenyl ring of another molecule [see overlay of Fig. 2(a)]. Neighboring chains are unable to form these stabilizing hydrogenlike bonds, and are possibly repelled by the positive charge distribution around the outer edges of the azobenzene chains (e.g., such a mechanism was suggested for 1-nitronaphthalene chains by Bohringer *et al.*).³

Molecule-surface interactions are likely van der Waals in nature and play two roles in the ordering of azobenzene molecules. First, at larger distance scales, molecule-surface interactions induce the azobenzene chains to order with respect to the large scale periodicity of the underlying herringbone surface reconstruction. This commensurability indicates a weak repulsion between azobenzene molecules and the domain boundaries between the fcc and hcp regions of the herringbone reconstruction (the surface ridges). This repulsion is strong enough to retain molecular commensurability even after the azobenzene molecules are converted from the straight phase to the zigzag phase via STM-tip manipulation. The second way in which the molecule-surface interaction influences the molecular ordering is in determining the allowed orientations of the straight azobenzene chains. Straight chains orient only in the three equivalent surface directions following the sixfold symmetry of the Au(111) hcp and fcc lattices.

In the high-coverage saturation regime, where molecules are tightly packed, intermolecular interactions dominate over molecule-substrate forces, and the resulting phases thus do

not order with the herringbone reconstruction. Surprisingly, however, the herringbone reconstruction does exert an influence on the behavior of azobenzene film vacancies. The vacancies appear to repel each other and the combination of mutual repulsion and herringbone surface interaction leads to the ordered structure. Vacancy repulsion might arise from electrostatic charge accumulation at the edges of short adjacent azobenzene chains, in a mechanism similar to straight chain repulsion in the low coverage regime.

In conclusion, we have observed a variety of ordered azobenzene molecular structures whose commensurability with the underlying Au(111) herringbone reconstruction is governed by a coverage-dependent competition between intermolecular and molecule-surface interactions. In the low coverage regime, intermolecular interactions determine the

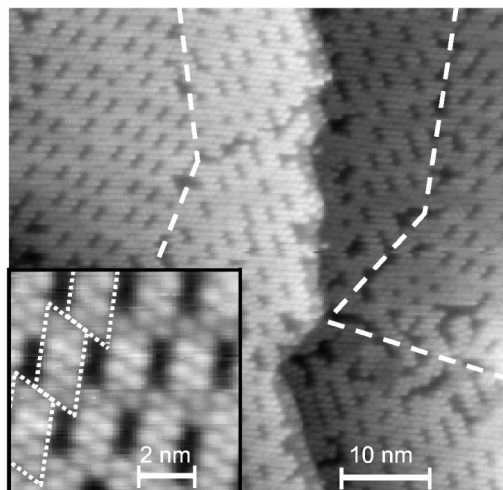


FIG. 4. STM image of 0.8 ML coverage of azobenzene on Au(111) surface (58×58 nm, 1.0 V, 25 pA, 35 K) showing ordered molecular vacancies (dark elongated depressions). The domains of aligned vacancies are separated by boundaries marked with dashed lines. Inset: close-up image (8×8 nm) of a vacancy domain showing the short-range molecular ordering of four-molecule-long chains (outlined by the dotted lines).

short-range order, leading to the formation of molecular chain structures. Long-range ordering of the chains, on the other hand, is dominated by the molecule-surface interaction and leads to chain orientations commensurate with the herringbone reconstruction. In the saturation coverage regime, intermolecular interactions determine both short- and long-range order, leading to molecular arrangements that are incommensurate with the herringbone reconstruction. At coverages only slightly below saturation, however, commensurability is recovered for azobenzene vacancies.

The coverage dependent structures observed here, in addition to the tip-induced phase conversion behavior, show that azobenzene molecular self-assembly can be controlled at the nanoscale.

We gratefully acknowledge useful discussions with J. M. J. Fréchet and Carine Edder. This work was supported in part by the Director, Office of Energy Research, Office of Basic Energy Science Division of the U. S. Department of Energy under Contract No. DE-AC03-76SF0098, and by NSF Grant No. CCR-0210176.

-
- ¹T. Yokoyama, S. Yokoyama, T. Kamikado, Y. Okuno, and S. Mashiko, *Nature (London)* **413**, 619 (2001).
- ²J. A. Theobald, N. S. Oxtoby, M. A. Phillips, N. R. Champness, and P. H. Beton, *Nature (London)* **424**, 1029 (2003).
- ³M. Bohringer, K. Morgenstern, W. D. Schneider, R. Berndt, F. Mauri, A. De Vita, and R. Car, *Phys. Rev. Lett.* **83**, 324 (1999).
- ⁴M. Bohringer, K. Morgenstern, W. D. Schneider, M. Wuhn, C. Woll, and R. Berndt, *Surf. Sci.* **444**, 199 (2000).
- ⁵S. Berner, M. de Wild, L. Ramoino, S. Ivan, A. Baratoff, H. J. Guntherodt, H. Suzuki, D. Schlettwein, and T. A. Jung, *Phys. Rev. B* **68** 115427 (2003).
- ⁶J. V. Barth, J. Weckesser, N. Lin, A. Dmitriev, and K. Kern, *Appl. Phys. A: Mater. Sci. Process.* **76**, 645 (2003).
- ⁷D. M. Walba, F. Stevens, N. A. Clark, and D. C. Parks, *Acc. Chem. Res.* **29**, 591 (1996).
- ⁸M. Taniguchi, H. Nakagawa, A. Yamagishi, and K. Yamada, *Surf. Sci.* **454**, 1005 (2000).
- ⁹T. A. Jung, R. R. Schlittler, and J. K. Gimzewski, *Nature (London)* **386**, 696 (1997).
- ¹⁰F. Moresco, G. Meyer, K. H. Rieder, H. Tang, A. Gourdon, and C. Joachim, *Phys. Rev. Lett.* **86**, 672 (2001).
- ¹¹M. Schunack, F. Rosei, Y. Naitoh, P. Jiang, A. Gourdon, E. Laegsgaard, I. Stensgaard, C. Joachim, and F. Besenbacher, *J. Chem. Phys.* **117**, 6259 (2002).
- ¹²S. M. Nie and S. R. Emery, *Science* **275**, 1102 (1997).
- ¹³G. Hoffmann, L. Libioulle, and R. Berndt, *Phys. Rev. B* **65** 212107 (2002).
- ¹⁴X. H. Qiu, G. V. Nazin, and W. Ho, *Science* **299**, 542 (2003).
- ¹⁵T. Hugel, N. B. Holland, A. Cattani, L. Moroder, M. Seitz, and H. E. Gaub, *Science* **296**, 1103 (2002).
- ¹⁶C. Zhang, M. H. Du, H. P. Cheng, X. G. Zhang, A. E. Roitberg, and J. L. Krause, *Phys. Rev. Lett.* **92** 158301 (2004).
- ¹⁷T. Umemoto, K. Ishikawa, H. Takezoe, A. Fukuda, T. Sasaki, and T. Ikeda, *Jpn. J. Appl. Phys., Part 1* **32**, L936 (1993).
- ¹⁸C. L. Feng, Y. J. Zhang, J. Jin, Y. L. Song, L. Y. Xie, G. R. Qu, L. Jiang, and D. B. Zhu, *Surf. Sci.* **513**, 111 (2002).
- ¹⁹S. Yasuda, T. Nakamura, M. Matsumoto, and H. Shigekawa, *J. Am. Chem. Soc.* **125**, 16430 (2003).
- ²⁰J. V. Barth, H. Brune, G. Ertl, and R. J. Behm, *Phys. Rev. B* **42**, 9307 (1990).
- ²¹C. J. Brown, *Acta Crystallogr.* **21**, 146 (1966).
- ²²C. S. Tsai, C. Su, J. K. Wang, and J. C. Lin, *Langmuir* **19**, 822 (2003).